Synthesis and characterization of A4[Re6Q8L6]@SiO2 red-emitting silica nanoparticles based on Re6 metal atom clusters (A = Cs or K, Q = S or Se, and L = OH or CN).

Tangi Aubert, Alexandra Y. Ledneva, Fabien Grasset, Koji Kimoto, Nikolay G. Naumov, Yann Molard, Noriko Saito, Hajime Haneda, Stéphane Cordier

Langmuir | 3b2 | ver.9 | 6/11/010 | 17:39 | Msc: la-2010-03784v | TEID: clr00 | BATID: 00000 | Pages: 6.29

Langmuir
Article

pubs.acs.org/Langmuir

Synthesis and Characterization of $A_4[Re_6Q_8L_6]@SiO_2$ Red-Emitting Silica Nanoparticles Based on Re_6 Metal Atom Clusters (A = Cs or K, Q = S or Se, and L = OH or CN)

Tangi Aubert,[†] Alexandra Y. Ledneva,[‡] Fabien Grasset,*[,†] Koji Kimoto,[§] Nikolay G. Naumov,[‡] Yann Molard,[†] Noriko Saito,[§] Hajime Haneda,[§] and Stéphane Cordier*[,†]

[†]*Université de Rennes 1, Unité Science Chimiques de Rennes, UMR 6226 CNRS-UR1, Campus de Beaulieu CS74205, F-35042 Rennes, Cedex, France,* [‡]*Nikolaev Institute of Inorganic Chemistry, Siberian Branch of the Russian Academy of Science, 3 Acad. Lavrentiev Prosp., 630090 Novosibirsk, Russia, and* [§]*National Institute for Materials Science, 1-1 Namiki, Tsukuba, Ibaraki 305-044, Japan*

Received September 21, 2010. Revised Manuscript Received October 27, 2010

Metal atom clusters constitute very promising candidates as luminophores for applications in biotechnology because they are nanosized entities offering robust luminescence in the near-infrared field (NIR). However, they cannot be used as prepared for biological applications because of potential toxic effects and quenching of the clusters' luminescence in aqueous media, and they therefore need to be dispersed in a biocompatible matrix. We describe herein the encapsulation of octahedral rhenium clusters, denoted as $A_4[Re_6Q_8L_6]$ (A = Cs or K, Q = S or Se, and L = OH or CN), in silica nanoparticles by a water-in-oil microemulsion process, paying particular attention to the clusters' stability. The obtained $A_4[Re_6Q_8L_6]@SiO_2$ nanoparticles are 30 nm in size with good monodispersity and a perfectly spherical shape, as shown by scanning electron microscopy (SEM). The presence of cluster units inside the silica matrix was evidenced by scanning transmission electron microscopy in annular dark-field mode (ADF-STEM). From the point of view of their optical properties, the $A_4[Re_6Q_8L_6]@SiO_2$ nanoparticles show red and NIR emission under UV excitation, even when dispersed in water. The evolution of the structural and luminescence properties of clusters before and after encapsulation was followed by Raman and photoluminescence spectroscopy.

1. Introduction

Many solid-state compounds, hybrid assemblies, and nanomaterials are based on octahedral metal atom clusters (M_6, with M = Mo, W, and Re) characterized by metal−metal bonds.[1,2] The M_6 cluster is surrounded by eight face-capping ligands (L^i, i = inner) to form a rigid $M_6Y^i{}_8$ core that is coordinated to six terminal ligands (L^a, a = apical) leading to an $M_6Y^i{}_8X^a{}_6$ neutral or anionic unit (Y = chalocogen and/or halogen; X = halogen). Solid-state materials based on such $M_6Y^i{}_8X^a{}_6$ units are easily synthesized at high temperature. They have been studied for many years for their interesting transport, catalytic, and electronic properties.[3−7] Many routes now afford soluble inorganic cluster precursors for soft chemistry synthesis.[8,9] Indeed, owing to their nanosized shape and their structural, redox, and photoluminescence properties, $M_6Y^i{}_8X^a{}_6$ anionic units constitute relevant building blocks for the elaboration of supramolecular assemblies, nanomaterials, and functionalized surfaces.[10−21] In solution or in inorganic (or organic) melts, apical ligands can be replaced by other ligands that are not stable under the synthesis conditions of the cluster. For instance, the reaction between $Cs_3[Re_6Q_7Br_7]\cdot H_2O$ (Q = S or Se) and melted pyrazine (pyz) leads to the formation of *fac*-$[Re_6Q^i{}_7Br^i(pyz)^a{}_3Br^a{}_3]\cdot xH_2O$ units that self-assembly via supramolecular interactions to built an original stable cluster-based hybrid framework.[16]

Many experimental and theoretical works report on the luminescence properties of Mo_6, W_6, and Re_6 cluster compounds.[22−27] It is worth noting that they emit in the red and near-infrared

*To whom correspondence should be addressed. E-mail: fabien.grasset@univ-rennes1.fr., stephane.cordier@univ-rennes1.fr.

(1) Cotton, F. A. *Inorg. Chem.* **1964**, *3*, 1217.
(2) Schäfer, H.; Schnering, H. G. *Angew. Chem.* **1964**, *76*, 833.
(3) Fischer, Ø. *Appl. Phys. A* **1978**, *16*, 1.
(4) Perrin, A.; Sergent, M.; Fischer, O. *Mater. Res. Bull.* **1978**, *13*, 259.
(5) Chevrel, R.; Sergent, M. Chemistry and Structure of Ternary Molybdenum Chalcogenides. In *Superconductivity in Ternary Compounds*; Fischer, Ø., Maple, M. P., Eds.; Topics in Current PhysicsSpringer-Verlag: Berlin, 1982; Vol. *32*; p 25.
(6) Tarascon, J. M.; Disalvo, F. J.; Murphy, D. W.; Hull, G. W.; Rietman, E. A.; Waszczak, J. V. *J. Solid State Chem.* **1984**, *54*, 204.
(7) Hilsenbeck, S. J.; McCarley, R. E.; Thompson, R. K.; Flanagan, L. C.; Schrader, G. L. *J. Mol. Catal. A: Chem.* **1997**, *122*, 13.
(8) Long, J. R.; McCarty, L. S.; Holm, R. H. *J. Am. Chem. Soc.* **1996**, *118*, 4603.
(9) Cordier, S.; Kirakci, K.; Méry, D.; Perrin, C.; Astruc, D. *Inorg. Chim. Acta* **2006**, *359*, 1705.
(10) Molard, Y.; Dorson, F.; Cîrcu, V.; Roisnel, T.; Artzner, F.; Cordier, S. *Angew. Chem., Int. Ed.* **2010**, *49*, 3351.
(11) Molard, Y.; Dorson, F.; Brylev, K. A.; Shestopalov, M. A.; Le Gal, Y.; Cordier, S.; Mironov, Y. V.; Kitamura, N.; Perrin, C. *Chem.—Eur. J.* **2010**, *16*, 5613.
(12) Selby, H. D.; Roland, B. K.; Zheng, Z. *Acc. Chem. Res.* **2003**, *36*, 933.
(13) Prabusankar, G.; Molard, Y.; Cordier, S.; Golhen, S.; Le Gal, Y.; Perrin, C.; Ouahab, L.; Kahlal, S.; Halet, J.-F. *Eur. J. Inorg. Chem.* **2009**, 2153.
(14) Méry, D.; Plault, L.; Ornelas, C.; Ruiz, J.; Nlate, S.; Astruc, D.; Blais, J.-C.; Rodrigues, J.; Cordier, S.; Kirakci, K.; Perrin, C. *Inorg. Chem.* **2006**, *45*, 1156.
(15) Méry, D.; Ornelas, C.; Daniel, M.-C.; Ruiz, J.; Rodrigues, J.; Astruc, D.; Cordier, S.; Kirakci, K.; Perrin, C. *C. R. Chim.* **2005**, *8*, 1789.
(16) Shestopalov, M. A.; Cordier, S.; Hernandez, O.; Molard, Y.; Perrin, C.; Perrin, A.; Fedorov, V. E.; Mironov, Y. V. *Inorg. Chem.* **2009**, *48*, 1482.
(17) Fabre, B.; Cordier, S.; Molard, Y.; Perrin, C.; Ababou-Girard, S.; Godet, C. *J. Phys. Chem. C* **2009**, *113*, 17437.
(18) Ababou-Girard, S.; Cordier, S.; Fabre, B.; Molard, Y.; Perrin, C. *ChemPhysChem* **2007**, *8*, 2086.
(19) Dybtsev, D.; Serre, C.; Schmitz, B.; Panella, B.; Hirscher, M.; Latroche, M.; Llewellyn, P. L.; Cordier, S.; Molard, Y.; Haouas, M.; Taulelle, F.; Férey, G. *Langmuir* **2010**, *26*, 11283.
(20) Beauvais, L. G.; Shores, M. P.; Long, J. R. *J. Am. Chem. Soc.* **2000**, *122*, 2763.
(21) Bennett, M. V.; Shores, M. P.; Beauvais, L. G.; Long, J. R. *J. Am. Chem. Soc.* **2000**, *122*, 6664.
(22) Gray, T. G.; Rudzinski, C. M.; Nocera, D. G.; Holm, R. H. *Inorg. Chem.* **1999**, *38*, 5932.
(23) Yoshimura, T.; Ishizaka, S.; Umakoshi, K.; Sasaki, Y.; Kim, H. B.; Kitamura, N. *Chem. Lett.* **1999**, 697.

(NIR) regions, which constitute a very interesting emitting window for biotechnology.[28,29] However, for such applications, it is required that no interaction occurs between clusters and tissues or biological media.

In this framework, we recently reported the synthesis of luminescent $Cs_2[Mo_6X_{14}]@SiO_2$ nanoparticles (X = Cl, Br, or I) via a water-in-oil microemulsion process wherein the cluster units are embedded in monodisperse silica nanoparticles.[30] Microemulsions are thermodynamically stable dispersions of water droplets in an oil phase, stabilized at the interface by surfactants molecules. Those water droplets, also called inverted micelles, are below 50 nm in size and constitute a suitable confined reaction medium for the synthesis of a wide variety of well-defined nanoparticles with controlled size and shape.[31,32] Using a similar approach, structured bifunctional magnetic and luminescent γ-Fe_2O_3-$Cs_2[Mo_6Br_{14}]@SiO_2$ nanoparticles were obtained by the introduction of maghemite nanocrystals at the core of the nanoparticles.[33] Whereas nowadays the luminophores developed for bioimaging and biolabeling technologies are mainly based on organic dyes,[34,35] inorganic quantum dots,[36] or lanthanide based nanocrystals,[37,38] metal atom clusters such as Re_6 clusters may offer complementary assets because they combine the important properties of perfectly reproducible nanosize, photostability, and NIR emission and do not show acute toxic effects.[39]

In addition to applications in biotechnology, functional silica particles can also find numerous applications in a wide range of fields such as photonics,[40] catalysis,[41] data storage devices,[42] cosmetics,[43] and so forth. In this article, we report the preparation of novel NIR-emitting nanoparticles obtained by the encapsulation of $[Re_6Q_8L_6]^{4-}$ cluster units (Q = S or Se and L = OH or CN) in silica nanoparticles by an adapted microemulsion process. Several kinds of clusters have been used to study the influence of the nature of inner and apical ligands on the cluster-embedding process as well as on the luminescence properties of embedded clusters. The Re_6 cluster precursors involved in this work were

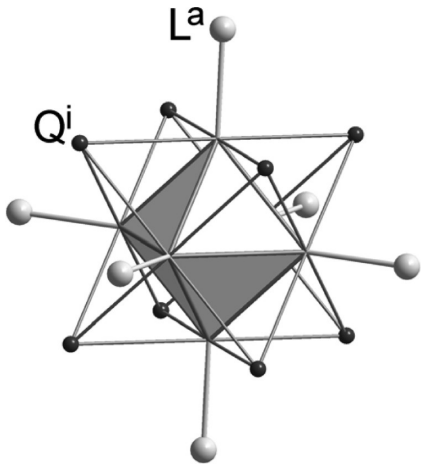

Figure 1. Schematic representation of a $Re_6Q^i{}_8L^a{}_6$ cluster unit. The Re_6 cluster core is represented as a gray octahedron. Inner ligands (Q^i = S or Se) are in the face-capping position, and apical ligands (L^a = OH, CN or Br) are in terminal positions.

$K_4[Re_6Q_8(OH)_6]$ (Q = S or Se), $Cs_4[Re_6S_8Br_6]$, and $Cs_{1.68}K_{2.32}[Re_6S_8(CN)_4(OH)_2]$. These Re_6 clusters are all luminescent in the red and NIR fields, with luminescence lifetimes of a few microseconds depending on the ligands.[25,44] It turns out that apical bromine in $[Re_6S^i{}_8Br^a{}_6]^{4-}$ units are quite labile under preparation conditions and are replaced by hydroxo groups during the embedding process but CN groups from $[Re_6S_8(CN)_4(OH)_2]^{4-}$ are not exchanged. We show that the luminescence properties of clusters are preserved after they are embedded in a silica matrix. An important finding is that although the luminescence of the $[Re_6Q_8L_6]^{4-}$ cluster units is originally quenched by oxygen in aqueous solutions, their luminescence properties are preserved in solution after they are embedded in silica nanoparticles.

2. Experimental Section

2.1. Chemicals. Tetraethoxysilane (TEOS) 98%, polyoxyethylene(4) lauryl ether (Brij30), and hydrobromic acid (HBr) 48% were purchased from Aldrich; *n*-heptane 99.0%, bromine (Br_2) 79.9%, sulfur (S) 99.5%, and aqueous ammonia solution (NH_4OH) 28% were purchased from Prolabo; ethanol (EtOH) 99.8% was purchased from Fluka; cesium chloride (CsCl) 99.9% and rhenium (Re) 99.997% were purchased from Alfa Aesar; and potassium hydroxide (KOH) 85% was purchased from Carlo Erba. All of the chemical reagents were used as received without further purification.

2.2. Synthesis of Re_6 Clusters. Hexanuclear rhenium clusters consist of six metal atoms forming an octahedron linked to eight chalcogen inner ligands (here S or Se) capping the faces of the octahedron, plus six apical ligands (here OH, Br, or CN) in the terminal positions of the octahedron. For illustration, a generic $Re_6Q^i{}_8L^a{}_6$ cluster unit is represented in Figure 1. The whole cluster unit is roughly 1 nm in size, depending on the nature of the apical ligands, and is negatively charged; it therefore needs to be charge balanced by counter cations in the solid state (here Cs or K). Most of the clusters are prepared by gas−solid or solid−solid synthesis and generally at high temperature. The cluster precursors used in this study were prepared according to well-known procedures reported in the literature.[45−47] They are briefly described in this section and summarized in Scheme 1.

(24) Yoshimura, T.; Ishizaka, S.; Sasaki, Y.; Kim, H. B.; Kitamura, N.; Naumov, N. G.; Sokolov, M. N.; Fedorov, V. E. *Chem. Lett*. **1999**, 1121.
(25) Yoshimura, T.; Matsuda, A.; Ito, Y.; Ishizaka, S.; Shinoda, S.; Tsukube, H.; Kitamura, N.; Shinohara, A. *Inorg. Chem*. **2010**, *49*, 3473.
(26) Gray, T. G. *Chem.—Eur. J*. **2009**, *15*, 2581.
(27) Grasset, F.; Molard, Y.; Cordier, S.; Dorson, F.; Mortier, M.; Perrin, C.; Guilloux-Viry, M.; Sasaki, T.; Haneda, H. *Adv. Mater*. **2008**, *20*, 1710.
(28) Contag, C. H.; Ross, B. D. *J. Magn. Reson. Imaging* **2002**, *16*, 378.
(29) Weissleder, R. *Nat. Biotechnol*. **2001**, *19*, 316.
(30) Grasset, F.; Dorson, F.; Cordier, S.; Molard, Y.; Perrin, C.; Marie, A. M.; Sasaki, T.; Haneda, H.; Bando, Y.; Mortier, M. *Adv. Mater*. **2008**, *20*, 143.
(31) Aubert, T.; Grasset, F.; Mornet, S.; Duguet, E.; Cador, O.; Cordier, S.; Molard, Y.; Demange, V.; Mortier, M.; Haneda, H. *J. Colloid Interface Sci*. **2010**, *341*, 201.
(32) Lopez-Quintela, M. A. *Curr. Opin. Colloid Interface Sci*. **2003**, *8*, 137.
(33) Grasset, F.; Dorson, F.; Molard, Y.; Cordier, S.; Demange, V.; Perrin, C.; Marchi-Artzner, V.; Haneda, H. *Chem. Commun*. **2008**, 4729.
(34) Ow, H.; Larson, D. R.; Srivastava, M.; Baird, B. A.; Webb, W. W.; Wiesner, U. *Nano Lett*. **2005**, *5*, 113.
(35) Ma, D.; Kell, A. J.; Tan, S.; Jakubek, Z. J.; Simard, B. *J. Phys. Chem. C* **2009**, *113*, 15974.
(36) Tan, T. T.; Selvan, S. T.; Zhao, L.; Gao, S.; Ying, J. Y. *Chem. Mater*. **2007**, *19*, 3112.
(37) Hu, H.; Xiong, L.; Zhou, J.; Li, F.; Cao, T.; Huang, C. *Chem.—Eur. J*. **2009**, *15*, 3577.
(38) Chen, G.; Ohulchanskyy, T. Y.; Kumar, R.; Ågren, H.; Prasad, P. N. *ACS Nano* **2010**, *4*, 3163.
(39) Choi, S.-J.; Brylev, K. A.; Xu, J.-Z.; Mironov, Y. V.; Fedorov, V. E.; Sohn, Y. S.; Kim, S.-J.; Choy, J.-H. *J. Inorg. Biochem*. **2008**, *102*, 1991.
(40) Dechézelles, J.-F.; Aubert, T.; Grasset, F.; Cordier, S.; Barthou, C.; Schwob, C.; Maître, A.; Vallée, R. A. L.; Cramail, H.; Ravaine, S. *Phys. Chem. Chem. Phys*. **2010**, *12*, 11993.
(41) Sreedhar, B.; Radhika, P.; Neelima, B.; Hebalkar, N.; Mishra, A. K. *Catal. Commun*. **2008**, *10*, 39.
(42) Hyun, C.; Lee, D. C.; Korgel, B. A.; de Lozanne, A. *Nanotechnology* **2007**, *18*, 055704.
(43) Jaroenworaluck, A.; Sunsaneeyametha, W.; Kosachan, N.; Stevens, R. *Surf. Interface Anal*. **2006**, *38*, 473.
(44) Brylev, K. A.; Mironov, Y. V.; Yarovoi, S. S.; Naumov, N. G.; Fedorov, V. E.; Kim, S.-J.; Kitamura, N.; Kuwahara, Y.; Yamada, K.; Ishizaka, S.; Sasaki, Y. *Inorg. Chem*. **2007**, *46*, 7414.
(45) Naumov, N. G.; Kim, S. J.; Virovets, A. V.; Mironov, Y. V.; Fedorov, V. E. *Bull. Korean Chem. Soc*. **2006**, *27*, 635.

Scheme 1. Summary of the Synthesis of Re_6 Inorganic Cluster Precursors[a]

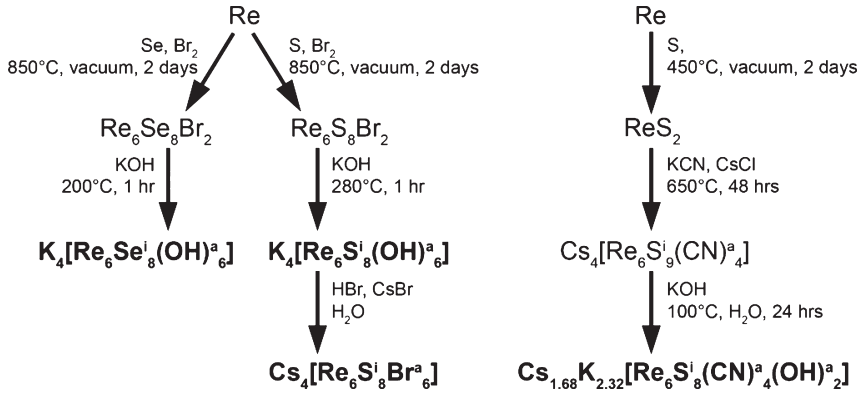

[a] In bold.

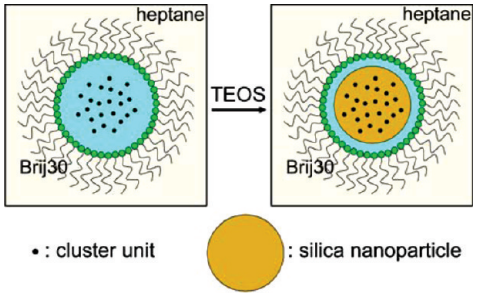

Figure 2. Schematic representation of the microemulsion process for the encapsulation of rhenium clusters inside a silica nanoparticle.

2.2.1. $K_4[Re_6Se_8(OH)_6]$ and $K_4[Re_6S_8(OH)_6]$.[47] Re, Se (or S), and liquid Br_2 were mixed in stoichiometric proportions, sealed under vacuum, and held at 850 °C for 2 days to obtain binary chalcogenide compound $Re_6Se_8Br_2$ (or $Re_6S_8Br_2$, respectively). This binary compound was then mixed with KOH and held at 200 °C (or 280 °C, respectively) in ambient air to obtain $K_4[Re_6Se_8(OH)_6]$ (or $K_4[Re_6S_8(OH)_6]$, respectively).

2.2.2. $Cs_4[Re_6S_8Br_6]$.[47] $Cs_4[Re_6S_8Br_6]$ was prepared by the reaction of $K_4[Re_6S_8(OH)_6]$ with CsBr in a water solution and with the pH adjusted to 2 with HBr.

2.2.3. $Cs_{1.68}K_{2.32}[Re_6S_8(CN)_4(OH)_2]$.[46] ReS_2 was prepared by the reaction of Re with S under vacuum at 450 °C for 2 days. $Cs_4[Re_6S_9(CN)_4]$ was then synthesized by the reaction of ReS_2 with KCN in the presence of excess CsCl at 650 °C for 48 h.[45] Finally, $Cs_{1.68}K_{2.32}[Re_6S_8(CN)_4(OH)_2]$ was obtained by the reaction of $Cs_4[Re_6S_9(CN)_4]$ with KOH in water, which had been boiled for 24 h.

2.3. Synthesis of $A_4[Re_6Q_8L_6]@SiO_2$ Nanoparticles. The $A_4[Re_6Q_8L_6]@SiO_2$ nanoparticles were prepared through a microemulsion process adapted from a previously reported synthesis for the encapsulation of nanocrystals (CeO_2 or $ZnFe_2O_4$)[48,49] or hexamolybdenum clusters in silica nanoparticles,[30] and this is illustrated in Figure 2. For all of the syntheses described here, the quantities of precursors used to form the final mixture were the following: 47 mL of heptane, 15 mL of Brij30, 1.6 mL of an aqueous cluster sol, 1.3 mL of ammonia, and 2 mL of TEOS. To create the microemulsion, heptane (oil phase) was first mixed with Brij30 (surfactant), and then an aqueous ammonia solution and an aqueous cluster sol were slowly added to the mixture. The aqueous cluster sol was obtained simply by solubilization of the cluster precursor in water. Depending on the solubility, the cluster concentration in the final aqueous phase could be adjusted. For $K_4[Re_6S_8(OH)_6]$ and $K_4[Re_6Se_8(OH)_6]$, this concentration was limited to 5 mM whereas it could reach 16 mM for $Cs_4[Re_6S_8Br_6]$ and 25 mM for $Cs_{1.68}K_{2.32}[Re_6(CN)_4(OH)_2]$. Once the microemulsion became a clear, stable solution, the silica precursor (TEOS) was added for the synthesis of the silica shell that occurred directly inside the aqueous nanodroplets already containing the cluster units. After the addition of TEOS, the reaction was stirred for 3 days and then the microemulsion was destabilized with ethanol and the nanoparticles were washed twice with an ethanol/heptane mixture (3:1 volume ratio) by centrifuging at 5000 rpm. Note that before destabilization of the microemulsion, the nanoparticle surface can be easily functionalized by the addition of a functional organosilane precursor. Finally, the nanoparticles could be either redispersed in solution (water or ethanol) or dried in ambient air.

2.4. Characterization of Materials. The external morphology of the nanoparticles was studied by field emission scanning electron microscopy (FE-SEM) with a Hitachi SU8000 working at an acceleration voltage of 10 kV. For FE-SEM observations, the nanoparticles were deposited on a silicon wafer and coated with a 3 nm layer of platinum using a JEOL JFC-1600 auto fine coater to enhance the conductivity of the sample. The microstructure of the nanoparticles and the distribution of the cluster units were observed using a scanning transmission electron microscope (Hitachi High-Technologies, HD-2300C) equipped with a spherical aberration corrector (CEOS GmbH, CESCOR) and working in annular dark-field mode (ADF-STEM).[50,51] The acceleration voltage was 200 kV, the convergent semiangle was 27.5 mrad, and the inner angle of the annular dark-field detector was 80 mrad. The spatial resolution of the instrument was about 0.1 nm. For ADF-STEM observation, the nanoparticles were dispersed on a thin carbon film whose thickness was about 6 nm. Investigations of the photoluminescence properties were performed in the solid state with a Jobin Yvon Fluorolog-3 fluorescence spectrometer (FL3-22, Horiba Jobin Yvon). The vibrational spectra were recorded with a Raman Bruker IFS 28 spectrometer equipped with a FRA 106 module. The excitation source was provided by a Nd:YAG laser working at 1064 nm. The power of the

(46) Naumov, N.; Ledneva, A.; Kim, S.-J.; Fedorov, V. *J. Cluster Sci.* **2009**, *20*, 225.
(47) Yarovoi, S. S.; Mironov, Y. V.; Naumov, D. Y.; Gatilov, Y. V.; Kozlova, S. G.; Kim, S.-J.; Fedorov, V. E. *Eur. J. Inorg. Chem.* **2005**, *2005*, 3945.
(48) Grasset, F.; Labhsetwar, N.; Li, D.; Park, D. C.; Saito, N.; Haneda, H.; Cador, O.; Roisnel, T.; Mornet, S.; Duguet, E.; Portier, J.; Etourneau, J. *Langmuir* **2002**, *18*, 8209.
(49) Grasset, F.; Marchand, R.; Marie, A. M.; Fauchadour, D.; Fajardie, F. *J. Colloid Interface Sci.* **2006**, *299*, 726.
(50) Kimoto, K.; Nakamura, K.; Aizawa, S.; Isakozawa, S.; Matsui, Y. *J. Electron Microsc.* **2007**, *56*, 17.
(51) Kimoto, K.; Asaka, T.; Nagai, T.; Saito, M.; Matsui, Y.; Ishizuka, K. *Nature* **2007**, *450*, 702.

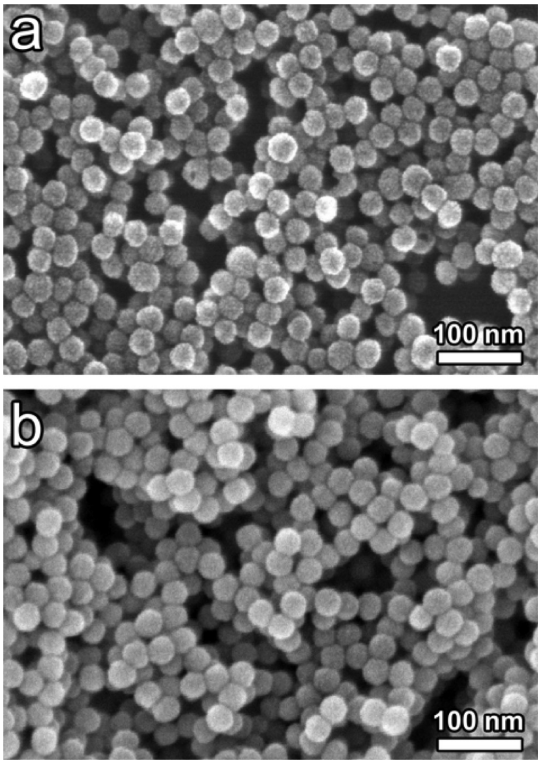

Figure 3. FE-SEM pictures of (a) $K_4[Re_6S_8(OH)_6]@SiO_2$ and (b) $Cs_{1.68}K_{2.32}[Re_6S_8(CN)_4(OH)_2]@SiO_2$ nanoparticles.

excitation was set to 30 mW in the case of $A_4[Re_6Q_8L_6]$ precursors to avoid burning the compound and 60 mW in the case of $A_4[Re_6Q_8L_6]@SiO_2$ nanoparticles in order to get a clear signal.

3. Results and Discussion

3.1. Synthesis. The synthesis of silica nanoparticles by microemulsion and its mechanism have already been widely studied and described in the literature.[52−54] It is a classical sol−gel process where an alkoxide precursor of silica (TEOS) is hydrolyzed, followed by the condensation of silica monomers. In the microemulsion, TEOS is first soluble in the heptane phase but is hydrolyzed by diffusion upon contact with the aqueous inverted micelles. The hydrolyzed silica monomers are then soluble in the aqueous phase, where they can condense via a base-catalyzed reaction.

The key point in the embedding of clusters in silica nanoparticles through this microemulsion process is to obtain stable cluster sols by avoiding the aggregation and precipitation of cluster units. Recall that for the preparation of the previously reported $Cs_2[Mo_6X_{14}]@SiO_2$ nanoparticles, the cluster units were solubilized in a water−ethanol mixture (1:1 v/v) and the pH was adjusted to 2 with bromic acid[30,31] in order to avoid the exchange of apical bromine by OH groups or water molecules and the subsequent precipitation of cluster units.[55] In the latter work, TEOS was added prior to ammonia and its hydrolysis was acid-catalyzed, thanks to the acidic aqueous cluster sol. Finally, ammonia was added to allow the base-catalyzed condensation of the silica matrix.

If the optical properties of Mo_6 clusters and Re_6 clusters exhibit some similarities, then the chemistry and reactivity of Mo_6-cluster-based units is different from that of Re_6. In particular, for rhenium cluster units containing hydroxyl groups in apical

(52) Osseo-Asare, K.; Arriagada, F. J. *Colloids Surf.* **1990**, *50*, 321.
(53) Osseo-Asare, K.; Arriagada, F. J. *J. Colloid Interface Sci.* **1999**, *218*, 68.
(54) Arriagada, F. J.; Osseo-Asare, K. *Colloids Surf., A* **1999**, *154*, 311.
(55) Sheldon, J. C. *J. Chem. Soc.* **1962**, 410.

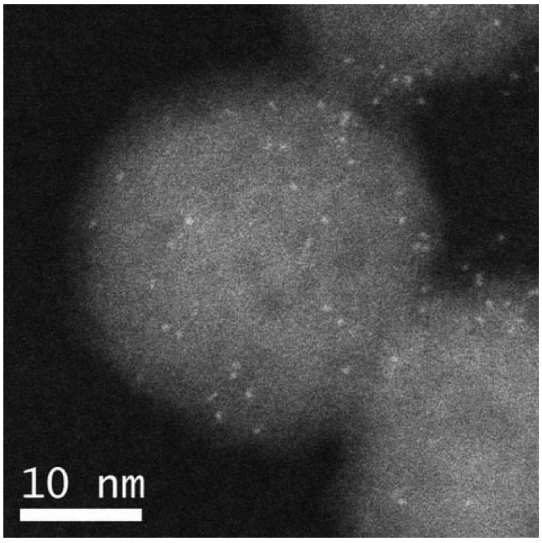

Figure 4. ADF-STEM pictures of $K_4[Re_6S_8(OH)_6]@SiO_2$ nanoparticles with discrete cluster units (bright spots).

positions, Brylev et al.[44] showed that, depending on the pH, hexahydroxo rhenium clusters $[Re_6Q_8(OH)_6]^{4-}$ can form aqua-hydroxo and hexaaqua cluster complexes with the general formula $[Re_6Q_8(H_2O)_n(OH)_{6-n}]^{n-4}$ (Q = S or Se; n = 0−6) because of the possible protonation of the apical −OH ligands. Such a phenomenon would induce changes in the composition and structure of the clusters, which might result in modifications of the luminescence characteristics or even precipitation of the clusters and therefore destabilization of the microemulsion. For instance, the $[Re_6Se_8(OH)_6]^{4-}$ cluster units remains stable in water at pH ∼14, whereas they fully precipitate at neutral pH because of the formation of $[Re_6Se_8(H_2O)_4(OH)_2]$ clusters.[44]

For the preparation of $A_4[Re_6Q_8L_6]@SiO_2$ nanoparticles, the cluster precursors were initially dissolved in water. Then, to prevent any change in the luminescence properties and to avoid precipitation of the clusters due to low pH, the microemulsions were prepared by adding ammonia to the heptane/Brij30 mixture prior to the aqueous cluster sol and prior to TEOS, so both the hydrolysis and condensation steps in the silica synthesis were base-catalyzed. The nanoparticles were then prepared according to the procedure described in section 2.3.

3.2. Nanoparticle Morphology and Microstructure. The as-prepared nanoparticles were observed by FE-SEM. The image analyses of $A_4[Re_6Q_8L_6]@SiO_2$ nanoparticles (Figure 3) showed F3 that they all exhibit a perfectly spherical, monodisperse morphology with an average diameter of 30 nm for the synthesis conditions described in section 2.3. Supplementary experiments showed that the size of the nanoparticles does not depend on the cluster concentration in the aqueous phase. To study the microstructure of the nanoparticles and confirm the encapsulation of the cluster units, the ADF-STEM technique is the only suitable tool because of the size of the cluster units (1 nm). Indeed, by detecting electrons scattered at high angles this technique provides what is known as *Z*-contrast images because atoms with high atomic numbers will be more scattered at high angle than atoms with lower atomic numbers. Thus, thanks to the large difference in electron numbers between the Re cluster core and Si or O from the silica matrix and the high spatial resolution of the STEM, it was possible to visualize the cluster units inside the nanoparticles. For example, Figure 4 shows an ADF-STEM image of $K_4[Re_6S_8(OH)_6]@SiO_2$ F4 nanoparticles where cluster units are visible as bright spots of about 1 nm in size. This image confirms that

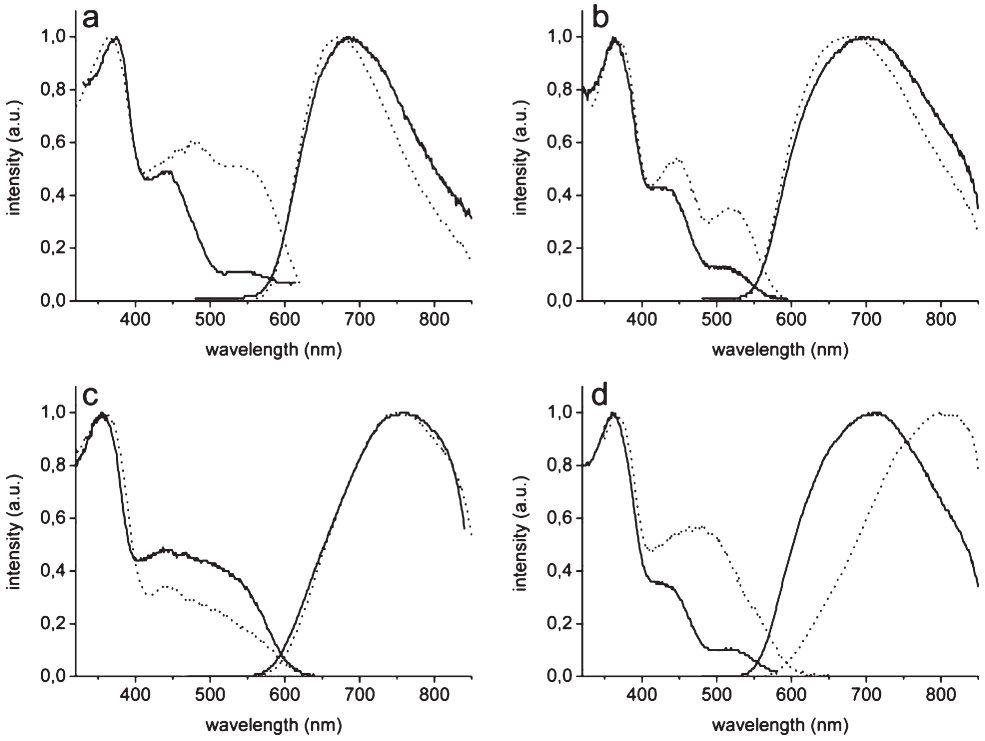

Figure 5. Normalized excitation and emission spectra (corrected signals) for both $A_4[Re_6Q_8L_6]$ cluster precursors (---) and $A_4[Re_6Q_8L_6]$@SiO_2 nanoparticles (—) for (a) $K_4[Re_6Se_8(OH)_6]$, (b) $K_4[Re_6S_8(OH)_6]$, (c) $Cs_{1.68}K_{2.32}[Re_6S_8(CN)_4(OH)_2]$, and (d) $Cs_4[Re_6S_8Br_6]$.

Table 1. Emission Maximum Wavelengths (λ_{em}) for $A_4[Re_6Q_8L_6]$ Cluster Precursors and $A_4[Re_6Q_8L_6]$@SiO_2 Nanoparticles

$A_4[Re_6Q_8L_6]$ cluster precursor	λ_{em} (nm)	$A_4[Re_6Q_8L_6]$@SiO_2 nanoparticles	λ_{em} (nm)
$K_4[Re_6S_8(OH)_6]$	680	$K_4[Re_6S_8(OH)_6]$@SiO_2	700
$K_4[Re_6Se_8(OH)_6]$	675	$K_4[Re_6Se_8(OH)_6]$@SiO_2	690
$Cs_{1.68}K_{2.32}[Re_6S_8(CN)_4(OH)_2]$	750	$Cs_{1.68}K_{2.32}[Re_6S_8(CN)_4(OH)_2]$@$SiO_2$	760
$Cs_4[Re_6S_8Br_6]$	800	$Cs_4[Re_6S_8Br_6]$@SiO_2	700

clusters were successfully encapsulated and homogeneously dispersed in the silica nanoparticles.

3.3. Luminescence Properties. The successful encapsulation of the cluster units in the silica nanoparticles was also evidenced by studying the luminescence properties of $A_4[Re_6Q_8L_6]$@SiO_2 nanoparticles. The luminescence properties were investigated in the solid state for both the $A_4[Re_6Q^i_8L^a_6]$ cluster precursors and the corresponding $A_4[Re_6Q_8L_6]$@SiO_2 nanoparticles. In Figure 5, the excitation and emission spectra for each type of cluster are plotted, and in Table 1, the wavelength values at the emission maximum (λ_{em}) are summarized.

The encapsulation of the $[Re_6Q^i_8(OH)^a_6]^{4-}$ (Q = Se or S) and $[Re_6S^i_8(CN)^a_4(OH)^a_2]^{4-}$ cluster units in the silica matrix resulted in a slight shift of the emission maxima after embedding, but the shape of the emission spectrum remained unchanged (Figure 5a−c). The emission maxima shifts, ranging from 10 to 20 nm, to higher wavelengths between solid-state precursors and the nanoparticles must be due to some perturbations of the molecular orbital diagram of $[Re_6Q^i_8L^a_6]^{4-}$ units after embedding. One could suspect a slight decrease in the energy gap between excited and fundamental states.

Some questions arose concerning the embedding of $[Re_6S^i_8Br^a_6]^{4-}$ units in silica nanoparticles. Indeed, the emission maxima for $[Re_6S^i_8Br^a_6]^{4-}$ units decreased from 800 nm in the $Cs_4[Re_6S_8Br_6]$ precursor to 700 nm after embedding in the silica matrix (Figure 5d). A closer look at the emission spectra shows that the shape of the emission spectrum of $Cs_4[Re_6S_8Br_6]$@SiO_2 nanoparticles (Figure 5d) and that of $K_4[Re_6S_8(OH)_6]$@SiO_2 nanoparticles (Figure 5b)

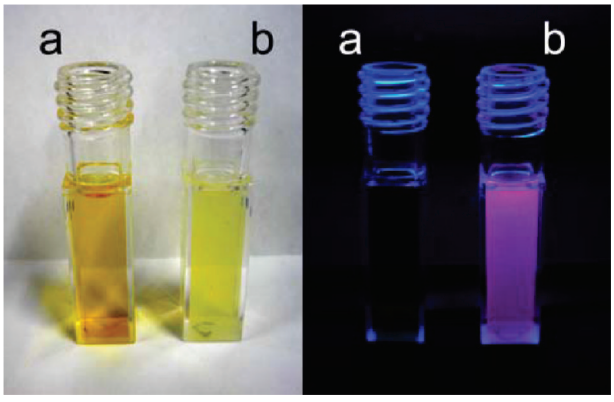

Figure 6. Aqueous solution of $[Re_6S_8(OH)_6]^{4-}$ clusters (a) before and (b) after embedding in silica nanoparticles, under daylight (left picture) and under UV irradiation at 365 nm (right picture).

match perfectly. This drastic change between the luminescence properties of the starting and embedded clusters can then be explained by an exchange of −Br apical ligands for −OH groups during the microemulsion process. In an attempt to avoid this structural modification, another synthesis of $Cs_4[Re_6S_8Br_6]$@SiO_2 nanoparticles was performed using acidic cluster sols (in which the pH was adjusted to 2 with HBr) either in a pure water solution or in a water/ethanol mixture (1:1 v/v). In both cases, the microemulsion stability was not affected but the resulting nanoparticles still show a luminescence shift to lower wavelengths, probably as a

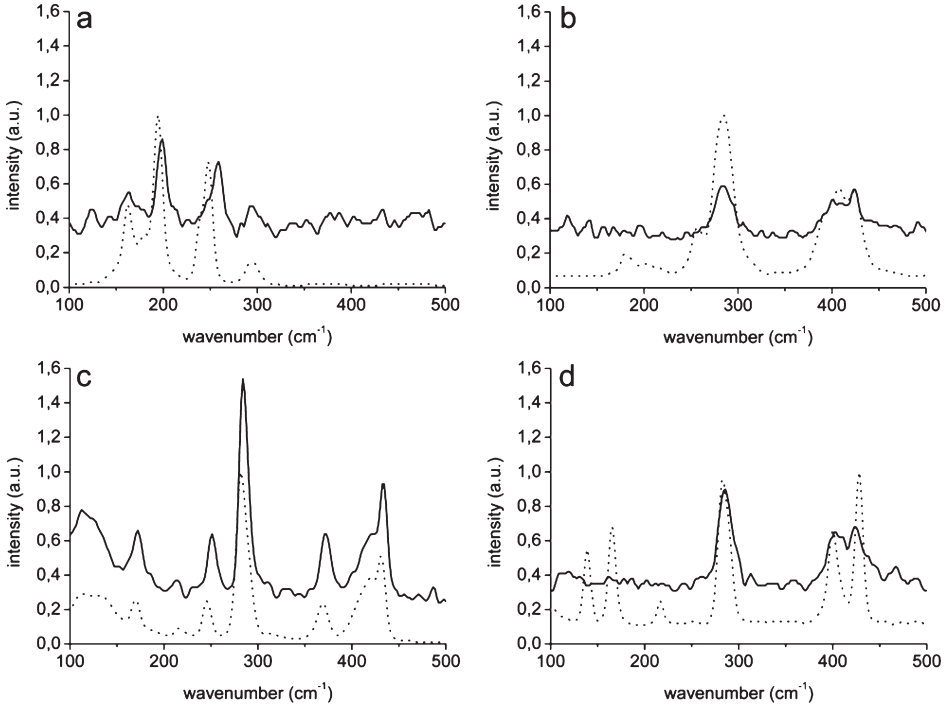

Figure 7. Raman spectra for both $A_4[Re_6Q_8L_6]$ cluster precursors (---) and $A_4[Re_6Q_8L_6]@SiO_2$ nanoparticles (—) for (a) $K_4[Re_6Se_8(OH)_6]$, (b) $K_4[Re_6S_8(OH)_6]$, (c) $Cs_{1.68}K_{2.32}[Re_6S_8(CN)_4(OH)_2]$, and (d) $Cs_4[Re_6S_8Br_6]$.

result of the exchange of apical bromine ligands for hydroxyl groups. Nonetheless and as previously mentioned, $Cs_2[Mo_6Br_{14}]@SiO_2$ nanoparticles prepared with a water/ethanol acidic cluster sol (pH adjusted to 2 with HBr) did not show any luminescence shift, meaning that no ligand exchange occurred during the encapsulation process. This indicates that $Re-Br^a$ bonds are much weaker than $Mo-Br^a$ bonds in an aqueous–alcoholic medium.

Concerning the excitation spectra, the encapsulation of the clusters in a silica matrix resulted in a lowering of the efficiency of excitation in the range of 400 to 600 nm. Once more in the case of $Cs_4[Re_6S_8Br_6]@SiO_2$ the excitation spectrum radically changed compared to that of the $Cs_4[Re_6S_8Br_6]$ precursor (Figure 5d) and perfectly match the excitation spectrum of $K_4[Re_6S_8(OH)_6]@SiO_2$ (Figure 5b). This finding again indicates that −Br apical ligands of $[Re_6S_8Br_6]^{4-}$ cluster units might be substituted for −OH groups during the microemulsion process.

The luminescence of clusters is usually quenched in solution because of the presence of solubilized oxygen. Indeed, it has been known for many years that excited octahedral clusters can be relaxed through the creation of singlet oxygen.[56] This quenching effect was successfully prevented by embedding the cluster units in silica nanoparticles. For illustration, Figure 6 shows a comparison between the luminescence properties of $[Re_6S_8(OH)_6]^{4-}$ cluster units in a water solution and after being embedded in silica nanoparticles under normal light and under UV irradiation at 365 nm. The $[Re_6S_8(OH)_6]^{4-}$ clusters show luminescence only when they are embedded in the silica matrix because they are then protected from the presence of solubilized oxygen and their luminescence is no longer quenched.

3.4. Raman Study. The vibrational properties of the $A_4[Re_6Q_8L_6]$ cluster precursors and those of $A_4[Re_6Q_8L_6]@SiO_2$ nanoparticles were investigated by Raman spectroscopy. The characterization of $M_6Q^i{}_8L^a{}_6$ units by Raman spectroscopy is not usual. The few published results show typical vibrations in the 50 to 400 cm^{-1} region. Their assignment is particularly tricky when the symmetry of the $M_6Q^i{}_8L^a{}_6$ units deviates from O_h symmetry. On the basis of the experimental and theoretical Raman investigations performed on $Re_6Q^i{}_8L^a{}_6$-cluster-unit-based compounds by Gray et al.,[57] it turns out that the Raman bands correspond to different kinds of $L^a{}_6$, $Q^i{}_8$, and Re_6 breathing modes.

The Raman spectra of the cluster precursors and of the corresponding cluster-based silica nanoparticles are represented in Figure 7. For all of the sulfide derivates (Figure 7b–d), the strong peaks at 280 and 430 cm^{-1} are easily identifiable in spectra of corresponding $A_4[Re_6Q_8L_6]@SiO_2$ nanoparticles and are respectively attributed to the T_{2g} vibrational mode and the A_{1g}-symmetric S_8 breathing mode of the clusters. For $Cs_{1.68}K_{2.32}[Re_6S_8(CN)_4(OH)_2]@SiO_2$, another strong peak is easily identifiable at 2120 cm^{-1} (data not shown here), which is due to the A_{1g} vibrational mode of the CN groups. Concerning $K_4[Re_6Se_8(OH)_6]@SiO_2$ nanoparticles (Figure 7a), the two intense peaks at 200 and 260 cm^{-1} can be observed and attributed to the T_{2g} and Se_8-A_{1g} vibrational modes, respectively, although they are slightly shifted (about 10 cm^{-1}) compared to the corresponding peaks in the starting cluster precursor. The spectra of $K_4Re_6Se_8(OH)_6@SiO_2$, $K_4Re_6S_8(OH)_6@SiO_2$, and $Cs_{1.68}K_{2.32}[Re_6S_8(CN)_4(OH)_2]@SiO_2$ nanoparticles exhibit all of the typical Raman signatures of the corresponding cluster precursor. This consequently confirms the successful encapsulation of the cluster units without significant structural modification. In contrast, the spectrum of $Cs_4[Re_6S_8Br_6]@SiO_2$ nanoparticles does not fully agree with the Raman signature of the $Cs_4[Re_6S_8Br_6]$ cluster precursor. Actually, the shape of the Raman spectrum for $Cs_4[Re_6S_8Br_6]@SiO_2$ nanoparticles (Figure 7d) is similar to the spectrum of the $K_4[Re_6S_8(OH)_6]@SiO_2$ nanoparticles (Figure 7b). Moreover, in Figure 7d the two intense peaks at 140 and 160 cm^{-1}, which were attributed to $Re-Br^a$ vibrational modes by Gray et al., are clearly

(56) Jackson, J. A.; Turro, C.; Newsham, M. D.; Nocera, D. G. *J. Phys. Chem.* **1990**, *94*, 4500.
(57) Gray, T. G.; Rudzinski, C. M.; Meyer, E. E.; Holm, R. H.; Nocera, D. G. *J. Am. Chem. Soc.* **2003**, *125*, 4755.

identifiable in the $Cs_4[Re_6S_8Br_6]$ compound but absent in the $Cs_4[Re_6S_8Br_6]@SiO_2$ nanoparticles. This observation shows that apical −Br ligands of $[Re_6S_8Br_6]^{4-}$ clusters are removed during the encapsulation process.

4. Conclusions

NIR-emitting nanoparticles were achieved by embedding hexarhenium clusters in silica nanoparticles using an adapted microemulsion process. $K_4[Re_6S_8(OH)_6]$, $K_4[Re_6Se_8(OH)_6]$, and $Cs_{1.68}K_{2.32}[Re_6S_8(CN)_4(OH)_2]$ were successfully encapsulated without any drastic changes in their luminescence properties. Attempts to embed $Cs_4[Re_6S_8Br_6]$ quaternary precursor in silica nanoparticles led to an exchange of apical −Br ligands during the microemulsion process, resulting in nanoparticles with physico-structural properties close to those obtained using the $K_4[Re_6S_8(OH)_6]$ precursor.

All of the cluster-based nanoparticles studied in this work are 30 nm in size with good monodispersity and exhibit a perfectly spherical shape. The cluster units are homogeneously dispersed inside the nanoparticles. A very important feature is that when embedded in silica the luminescence of the clusters is not quenched by oxygen in solution.

Toxicological studies are currently performed to evaluate the toxicological potential of such nanoparticles. If the silica shell efficiently proves to prevent any toxic effect from the metal atom clusters, then such material will have numerous potential applications in the field of biotechnology.

Acknowledgment. This work was supported by the University of Rennes 1, CNRS, and joint Japan-RFBR grant 09-03-92100-ЯФ_a. Christiane Perrin is acknowledged for helpful discussions and local management of the PECO-NEI & ECONET programs. A.Y.L. and N.G.N. are grateful to the PECO-NEI & ECONET programs for research grants at the University of Rennes 1. T.A. thanks Région Bretagne for a Ph.D. grant and the Collège Doctoral Franco-Japonais for a research grant at NIMS. We thank Dr. K. Hasegawa (NIMS) for supplying the SEM images and Dr. F. Paul (University of Rennes 1) for the Raman measurements.